

Impact of Modelling Assumptions on the Voltage Stability Assessment of Active Distribution Grids

Boricic, Aleksandar; Torres, Jose L. Rueda; Popov, Marjan

DOI

[10.1109/ISGT-Europe47291.2020.9248764](https://doi.org/10.1109/ISGT-Europe47291.2020.9248764)

Publication date

2020

Document Version

Final published version

Published in

2020 IEEE PES Innovative Smart Grid Technologies Europe (ISGT-Europe)

Citation (APA)

Boricic, A., Torres, J. L. R., & Popov, M. (2020). Impact of Modelling Assumptions on the Voltage Stability Assessment of Active Distribution Grids. In *2020 IEEE PES Innovative Smart Grid Technologies Europe (ISGT-Europe): Proceedings* (pp. 1040-1044). [9248764] IEEE . <https://doi.org/10.1109/ISGT-Europe47291.2020.9248764>

Important note

To cite this publication, please use the final published version (if applicable).
Please check the document version above.

Copyright

Other than for strictly personal use, it is not permitted to download, forward or distribute the text or part of it, without the consent of the author(s) and/or copyright holder(s), unless the work is under an open content license such as Creative Commons.

Takedown policy

Please contact us and provide details if you believe this document breaches copyrights.
We will remove access to the work immediately and investigate your claim.

Green Open Access added to TU Delft Institutional Repository

'You share, we take care!' - Taverne project

<https://www.openaccess.nl/en/you-share-we-take-care>

Otherwise as indicated in the copyright section: the publisher is the copyright holder of this work and the author uses the Dutch legislation to make this work public.

Impact of Modelling Assumptions on the Voltage Stability Assessment of Active Distribution Grids

Aleksandar Boricic
Delft University of Technology
Intelligent Electrical Power Grids
Delft, The Netherlands
A.Boricic@tudelft.nl

Jose L. Rueda Torres
Delft University of Technology
Intelligent Electrical Power Grids
Delft, The Netherlands
J.L.RuedaTorres@tudelft.nl

Marjan Popov
Delft University of Technology
Intelligent Electrical Power Grids
Delft, The Netherlands
M.Popov@tudelft.nl

Abstract—Renewable energy sources (RES) penetrate power grids at all voltage levels. A large number of RES units are connected to medium-voltage (MV) and low-voltage (LV) levels resulting in a significant share of overall generation. Therefore, the dynamic behavior of such distribution grids should be thoroughly examined. The goal of this paper is to show how various changes in the composition of the dynamic power flows interact with Low-Voltage Ride Through (LVRT) requirements, and how they affect the very important aspect of the RES-penetrated grids – voltage stability. The analysis is performed on a selected network, which is modeled with real grid data. The concluding concepts, however, are applicable for any distribution grid topology with a large number of distributed energy resources (DER). The results show essential grid details that should be modeled more precisely. This paper also addresses the level of complexity needed to obtain accurate results. Models are generally always imperfect and therefore, having more detailed data for a specific study is of the uttermost importance.

Keywords— *Distributed energy resources, Modelling, Voltage stability, Low-Voltage Ride Through (LVRT), Renewable energy*

I. INTRODUCTION

The resilience of distribution grids, which include a high amount of renewable energy becomes a very important factor for grid stability. Imposed LVRT requirements are the correct measures to successfully withstand the disturbances in order to continue the operation without a loss of generation, however, those requirements are not so easily met in a distribution grid. Not all the DER should comply with these demands, and this depends on their commission date and installed capacity. The general LVRT requirements for generators are described in [1]. However, these codes are mainly focused on the larger RES, i.e. type B, C and D. Smallest type sources, i.e. type A, are generally described in the country-specific normative. In the Netherlands, the requirements of the generating plants are defined according to [2] and [3] and the details are presented in Section II.

Sometimes it is difficult to fully meet the LVRT requirements and this is mainly because of the fault clearing time of the protection systems in a distribution grid. While transmission grids utilize modern and fast protection systems, which successfully operate within several cycles (e.g. distance protection), distribution grids usually rely on Overcurrent Relays (OCRs). Even though OCRs usually locate and isolate the faults successfully, their operating times are longer, mainly due to the necessity of introducing time delays to provide the required selectivity. This implies that the distribution relays may have longer operating times than transmission relays. Therefore, interactions between protection coordination and LVRT requirements in a distribution grid is challenging, and also very important to analyse, as shown in [4].

Lastly, DG units may become transiently unstable when they operate during longer LVRT-imposed voltage dips. Balancing these effects together can be challenging, resulting in a high chance of misoperation or suboptimal settings [5].

Model-specifics such as voltage-power dependence of loads and induction motors play a significant role in the voltage trajectory during and after a disturbance. While these have been so far extensively explored [6-8], their interaction with LVRT requirements is still unclear. This paper further explores this relation and proposes robust overall guidelines for the modelling assumptions and its implications, by focusing on the highly RES-penetrated distribution grids. Furthermore, a critical approach in assessing how these combined effects can affect the post-fault voltage stability is applied for RES-dominated grids based on a literature review.

This paper is organized as follows. Section II briefly explains the concept of voltage stability phenomena, with a specific focus on each of the elements used in the modelled distribution grid. Section III introduces the synthetic model of a part of the Dutch distribution grid, created in DIGSILENT PowerFactory 2018, to simulate several scenarios dealing with voltage stability matters. Section IV shows the simulation results and analysis. Section V deals with the implications of long-term voltage instability and Section VI presents the final recommendations and conclusions.

II. VOLTAGE STABILITY – PHENOMENON AND INFLUENCES

Voltage stability is defined as the ability of a power system to maintain steady and acceptable voltages at all buses in the system under normal operating conditions and after being subjected to a disturbance [9]. It is usually divided into two groups - short-term and long-term voltage stability. This paper focuses on the initial short-term voltage stability, i.e. during-disturbance voltage trajectory with LVRT implications. The influence on long-term voltage stability is further discussed in Section V. Some of these impacts are studied extensively in a recent study [8].

A. Load modelling influence

Load modelling and its influence on the voltage stability was researched carefully in the past, e.g. in [10]. Therefore, this paper will only merely indicate the main conclusions of the aforementioned studies.

Load models are generally divided into static and dynamic models. Static models exhibit the same voltage-power dependency throughout a disturbance and recovery (voltage exponents α_p and α_Q , see e.g. [10]) and dynamic models show varying dependency over time. The analysis in this paper will be performed with static load models only, and the implications of dynamic behavior will be addressed in Section V.

B. Induction motors

The presence of induction motors in a distribution grid is a common practice, and their effects on the voltage profile are also known, [6], [7], [10]. The induction machine, in comparison to the static load, provides larger fault current resulting in a more severe voltage decrease. This is an important matter when dealing with the DER and their corresponding LVRT requirements.

After the fault is cleared, the induction motor enters into a recovery phase, where the fault clearing time and the motor terminal voltage determine whether a stable operation or a stalling mode will take place. The implications of a stalling motor will be addressed in Section V.

C. Combined Heat&Power (CHP) Plants

The grid in question for this study encompasses a significant number of CHP plants. These plants primarily provide heat for a residential or agricultural need, whilst the surplus of electric energy is supplied to the grid. The plants mostly make use of Synchronous Generators (SG) driven by a gas or a steam turbine, even though other types of generators can also be used. For the analysis presented in this paper, SG-based CHP units are used.

CHP plants in the grid are connected to the 10 kV busbar with installed power ranging from several hundreds of kilowatts up to several megawatts. They are connected to the MV grid, and their LVRT requirements are reported in [3]. Figure 1 shows the LVRT voltage-time curve for SG units.

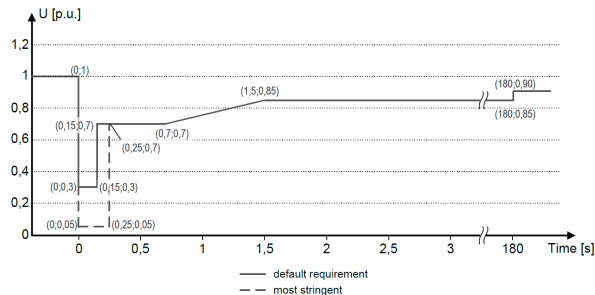


Fig. 1. LVRT Requirements, MV-connected SG in the Netherlands [3]

SG-based DER should comply with the default curve requirements, and the Distribution System Operator (DSO) is free to make them stricter if needed, as long as the most stringent curve is not exceeded, as shown in Figure 1.

D. Double-Fed Induction Generators (Wind Turbines)

Wind power is, alongside with solar power, the main driver of the energy transition. It is installed in large and small capacities, in both distribution and transmission grids. Countries like the Netherlands, which have strong and constant winds alongside its territories, focus largely on this type of RES.

In the grid which is studied in this paper, most wind turbines are connected to the low voltage level (0.4 kV). Depending on their size and commissioning date, some of these turbines (but not all) should follow the specific LVRT demand [2]. The exact number is often difficult to determine, and therefore model assumptions are used. Those which should comply with LVRT requirements need to adhere to the voltage-time curve as it can be seen in Figure 2.

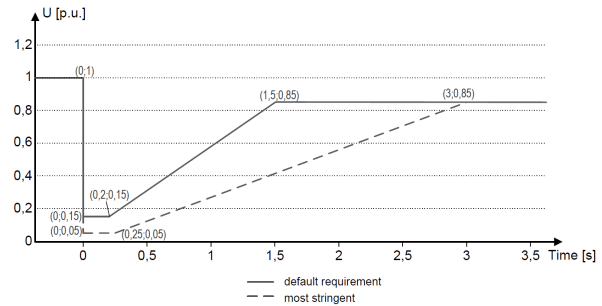


Fig. 2. LVRT Requirements, LV-connected non-SG in the Netherlands [2]

Similarly to Figure 1, Figure 2 contains the default requirements which should be met, however, the DSO determines where exactly between the two curves, the default and the most stringent one, the actual curve will be located.

III. CASE-STUDY MODEL

The observed grid is a 50 kV distribution grid containing several substations with high RES penetration [11]. However, to study the effects of the four elements discussed in Section II more precisely, one of the substations is extracted and remodelled in PowerFactory environment as it is shown in Figure 3.

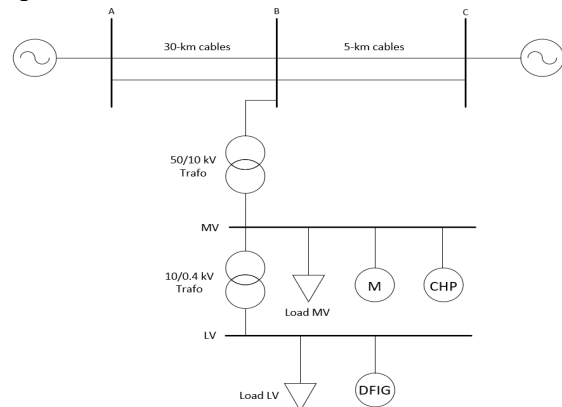


Fig. 3. Single-line diagram of the Case-Study Grid

The value of the total power on the 50/10 kV transformer, hereby defined as the net load, is a known parameter for the DSO. However, the composition of that load and its voltage dependence is often based on assumptions. Here, we will address how the same net load, but a different composition of it, affects during- and after-disturbance voltage trajectory, with the focus on voltage stability implications.

Passive grid elements, i.e. cables and transformers, are modelled based on the available grid data [12]. For the DER, aggregated models are used, which are directly connected to the busbars. Since the actual grid has continuations with more similar substations, two strong grids are connected to the remote ends, with their short-circuit power set to 400 MVA.

The components connected to the 10 kV (MV busbar) level and 0.4 kV (LV busbar) level are modelled in more detail. Loads are modelled as complex voltage-dependent PowerFactory loads, divided equally between LV and MV busbar. Induction motors are modelled as aggregated units by using ABB 750 KW PowerFactory Induction Machine models. The CHP plant connected to the 10 kV level is also

modelled with an aggregated model in a way to provide a power of 26 MVA based on the DSO's data. The generator control consists of an automatic voltage regulator (AVR) and a governor with standard Power Factory parameters. DFIG wind turbines are modelled as four aggregated units of 3 MW each, with detailed parameters and control based on the generic PowerFactory data according to [11] and [12]. A sensitivity analysis concerning these control parameters is a topic of future research by the authors and is hereby not included.

Under-voltage protection of generators is designed in such a way to follow the default LVRT requirements during the disturbances as shown in Figures 1 and 2. When the point-of-connection (PoC) voltage during the fault drops below the corresponding LVRT curve, CHP and DFIG sources are set to disconnect after 100ms.

IV. SIMULATION RESULTS

To evaluate how the composition of net load affects the voltage behaviour, several scenarios are created in a way to effectively capture and demonstrate interactions of load modelling and induction motors with LVRT requirements in a distribution grid.

For all the scenarios, the net load on the 50/10 kV transformer is $S=10.1+2.5j$ MVA, and it is supplied to the 50 kV grid. This is usual for the observed grid since the DER production is often higher than the local consumption. The reader should keep in mind that the grid losses are neglected, and this may lead to a small disagreement between the net load and the total load composition. Anyhow, this does not affect the simulation results.

A disturbance is initiated as a 3-phase short circuit that occurs in one of the A-B cables, 3 km away from busbar B. The fault inception time is at $t=1s$, and it is cleared after $\Delta t=0.7s$.

A. Scenario 1

For the initial scenario, the net load composition is shown in Table I, and it is largely based on [11] and [12]. This will be used as a reference comparison case for other scenarios.

TABLE I – SCENARIO 1 POWER FLOW PER ELEMENT

Element	Power Flow (MVA)
DFIG	$12 + 2.4j$
CHP	$10 + 4j$
Load ($\alpha_p = 1; \alpha_Q = 1$)	$12 + 3.5j$
Motors	0

Figure 4 shows the voltage on busbars LV and MV.

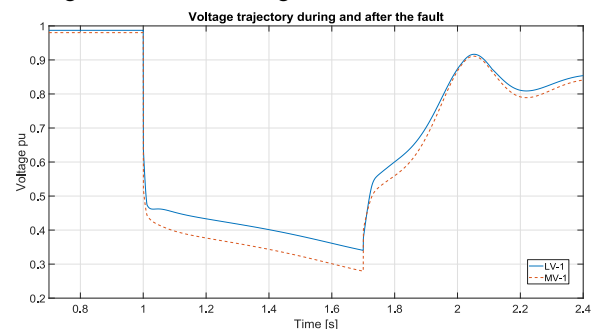


Fig. 4. MV and LV Scenario 1 voltage trajectory during and after the fault

From Figure 4, it can be seen that the voltage drops sharply when the fault initiates ($t=1s$), and then gradually decreases until the fault is cleared at $t=1.7s$ followed by a voltage recovery. No DER plants got disconnected in this case. The voltage at the MV busbar is slightly lower, as expected since this busbar is closer to the fault location.

B. Scenario 2

For the second scenario, the composition of the net load is shown in Table II.

TABLE II – SCENARIO 2 POWER FLOW PER ELEMENT

Element	Power Flow (MVA)
DFIG	$12 + 2.4j$
CHP	$10 + 4j$
Load ($\alpha_p = 1.6; \alpha_Q = 1.8$)	$12 + 3.5j$
Motors	0

The only difference, in this case, is in the voltage-power dependency of the load, which is increased to 1.6 and 1.8 for the active and the reactive power, respectively. These values are based on more precise grid data as per the model in [12].

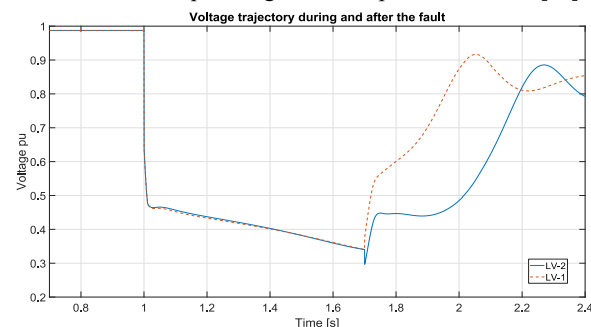


Fig. 5. Scenario 2 (LV-2) versus Scenario 1 (LV-1) voltage trajectory

The effect of this change is only visible after the fault is cleared. This has to do with the PowerFactory short-circuit calculation method, which assumes the same impedance load model when calculating the fault current, which is in line with the standard IEC 60909 [13]. Hence, this scenario will only be used for Section V; long-term voltage implications. For short-term events, the experience shows that the higher voltage-power dependency is beneficial for the system since the load effectively reduces when the voltage drops. For other scenarios, a voltage dependency of 1.6 and 1.8 for the active and the reactive power, respectively, is used for the load.

C. Scenario 3

For the third scenario, the composition of the net load is shown in Table III.

TABLE III – SCENARIO 3 POWER FLOW PER ELEMENT

Element	Power Flow (MVA)
DFIG	$12 + 2.4j$
CHP	$10 + 4j$
Load ($\alpha_p = 1.6; \alpha_Q = 1.8$)	$6 + 1.75j$
Motors	$6 + 1.75j$

In this scenario, 50% of the static load has been replaced with induction motors, to show their effect on the voltage behaviour. The change of the slope of the voltage drop during the fault is evident, and this is in line with previous explanations since an induction machine behaves as a constant power load and further reduces the PoC voltage.

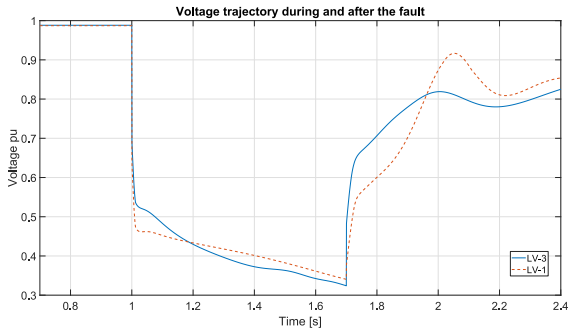


Fig. 6. Scenario 3 (LV-3) versus Scenario 1 (LV-1) voltage trajectory

D. Scenario 4

For the fourth scenario, the composition of the net load is shown in Table IV.

TABLE IV – SCENARIO 4 POWER FLOW PER ELEMENT

Element	Power Flow (MVA)
DFIG (75% LVRT)	$12 + 2.4j$
CHP	$10 + 4j$
Load ($\alpha_p = 1.6; \alpha_Q = 1.8$)	$12 + 3.5j$
Motors	0

It is assumed that a quarter of the DFIG units do not have to (or cannot) comply with the LVRT requirements. The disconnection occurs 150ms after the fault.

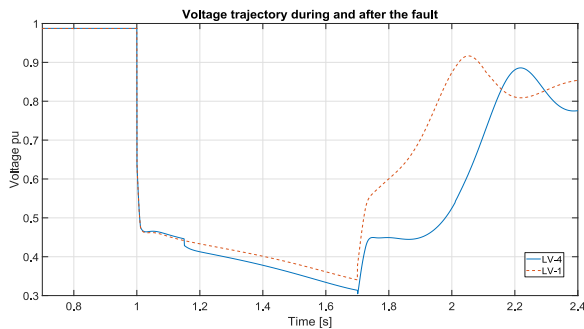


Fig. 7. Scenario 4 (LV-4) versus Scenario 1 (LV-1) voltage trajectory

In Figure 7, voltage LV-4 drops more than the voltage shown in the LV-1 case, as expected due to the 25% of the DFIG disconnection. However, this does not lead to any further disconnections of LVRT-compliant DER.

E. Scenario 5

For the final scenario, the composition of the net load is shown in Table V.

TABLE V – SCENARIO 5 POWER FLOW PER ELEMENT

Element	Power Flow (MVA)
DFIG (75% LVRT)	$12 + 2.4j$
CHP	$10 + 4j$
Load ($\alpha_p = 1.6; \alpha_Q = 1.8$)	$6 + 1.75j$
Motors	$6 + 1.75j$

In this final case, all the scenarios are effectively combined. Hence, 25% of the DFIG generation fails to comply with the LVRT demand and disconnects after 150ms, whilst 50% of the total static load is replaced by induction motors. The resulting graph presented in Figure 8 shows the main point of the analysis.

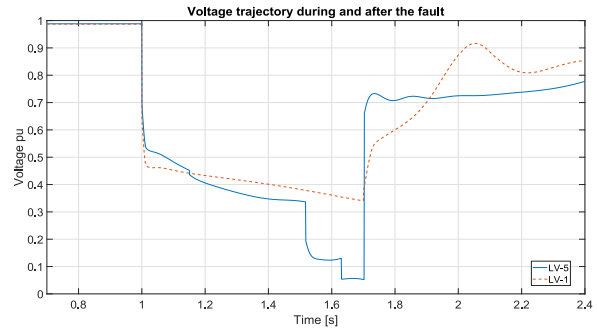


Fig. 8. Scenario 5 (LV-5) versus Scenario 1 (LV-1) voltage trajectory

After the fault, the voltage rapidly drops as a result of the motor current increase, followed by 25% of the DFIG disconnection in the same way as it was in scenario 4. However, these two effects together lead to a significantly stronger voltage drop, and at $t=1.516s$, the entire CHP generation is disconnected. This causes voltage collapse resulting in a complete DFIG disconnection at $t=1.628s$. Figure 9 shows the simulated voltage on the MV busbar for this scenario compared to that simulated in scenario 1.

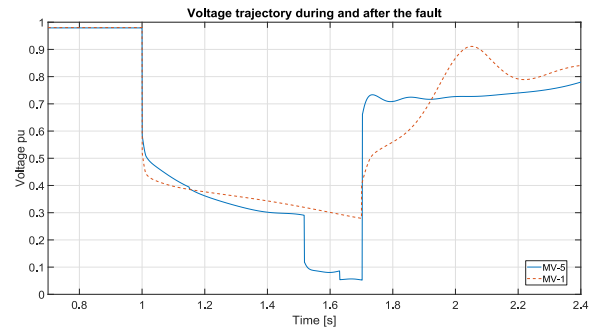


Fig. 9. Scenario 5 (MV-5) versus Scenario 1 (MV-1) voltage trajectory

At $t=1.416s$ in Figure 9, the voltage of the MV busbar drops below 0.3 per unit. As per Figure 1, this value is below the LVRT requirements and therefore, CHP disconnects after 100ms, whilst DFIG disconnects 100ms after the LV busbar voltage drops below the corresponding LVRT curve (shown in Figure 2). Figure 10 shows all the scenarios for the voltage at the LV busbar and also indicates the worst-case scenario.

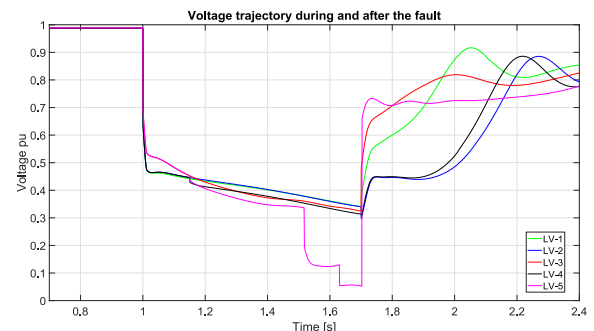


Fig. 10. LV busbar voltage trajectory for all five scenarios

Another important detail is the post-fault voltage in scenario 5 being notably lower in comparison to the other scenarios. Therefore, it is obvious that grid model details are very important for the evaluation of the resulting post-fault voltage profile. This is further addressed in Section V.

V. LONG-TERM VOLTAGE STABILITY IMPLICATIONS

Performed simulations confirm the theoretical expectations mentioned in Sections I and II, i.e. net load composition can significantly affect grid behaviour during the fault. However, the main implications may happen in the post-fault phase, where several factors should be considered.

A. Disconnection of DER plants

When a significant number of DER plants are disconnected, the net power direction can effectively reverse during the post-fault period. Considering that there are many similar substations which may behave comparably, the overall power demand from the 50 kV grid perspective can significantly increase after the fault. This may further reduce the post-disturbance voltage, leading to dangerously low voltage levels. This is especially important for cable grids, since their X/R ratio is generally lower than one, causing the voltage to be more sensitive to active power changes [7].

B. Load recovery process

Loads are playing a major role in voltage stability, and their restoration is of high importance. For instance, when a grid contains a large number of thermal loads, they tend to behave as dynamic loads, restoring their active power on even lower voltage levels, which results in higher load current. This increases the stress on the grid, ultimately demanding more power and leading to further voltage reduction [10].

C. On-Load Tap Changer (OLTC) operation

After the fault is cleared, the OLTCs in the grid attempt to restore the voltage to the nominal value. However, if the grid is unable to provide enough power to sustain these new voltage values, a downward spiral starts. OLTCs change tap positions in an attempt to improve the voltage level, and it effectively increases the load (as per load-voltage dependency). The operation continues until the OLTCs reach their last tap position, or the voltage collapses [6] [7].

D. Over-Excitation Limiters (OXL)

Most of the synchronous generators have limitations in their maximum excitation level since otherwise, the excitation winding would overheat. These limitations reduce the excitation after some time, usually following the inverse current-time characteristic, capping the supplied reactive power, and further boosting the voltage drop [7].

E. Motor Stalling

When a motor voltage is low for a longer duration, it may begin to stall. Motor stalling leads to motor speed reduction followed by an increase of the slip, which results in increased reactive power consumption until the motor fully stops [6].

F. Cascading Faults

Many major blackouts are events which begin with one fault evolving into a cascading event. While two unrelated faults occurring at the same time are statistically very unlikely, one fault triggering another fault is, on the other hand, a very common scenario. When a part of the grid is disconnected, the overall stress on the rest of the grid increases. Hence, it should be considered that one disturbance might cause a series of disconnections along the entire distribution grid.

While the effects are here described separately, the major concern, once again, is in their interaction. Voltage instability rarely has a single root cause. Interactions between all these phenomena develop rapidly, and DSO/TSO engineers might have difficulties in voltage deterioration prevention.

VI. CONCLUSION

The paper demonstrates how the interactions of different load compositions and LVRT requirements of DER can be a bottleneck in a distribution grid resilience. This is particularly relevant for largely RES-penetrated grids. The implication of this conclusion is the necessity of addressing load models more precisely, especially if they include induction machines. Furthermore, DER undervoltage operation, dictated by country-specific LVRT requirements, should be introduced accurately in the model, while keeping in mind the possibilities of noncompliance due to protection (and any other) limitations. Lastly, the paper summarized and presented implications for voltage stability, which require further addressing and research. The last thought we mention here is that modern solutions based on synchrophasors measurement and control strategies may be an advisable way to tackle these instability concerns, avoiding dangerous grid states. This shall be a topic of future studies by the authors.

ACKNOWLEDGMENT

This work was financially supported by Dutch Scientific Council NWO in collaboration with TSO TenneT, DSOs Alliander, Stedin, Enduris, VSL and General Electric in the framework of the Energy System Integration & Big Data program under the project "Resilient Synchroreasurement-based Grid Protection Platform, no. 647.003.004"

REFERENCES

- [1] The European Commission, "Commission Regulation (EU) 2016/631 – Establishing a Network Code on Requirements for Grid Connection of Generators", 2016
- [2] Nederlandse Norm NEN-EN 50549-1, "Requirements for Generating plants to be connected in parallel with distribution networks – Part 1: Connection to a LV distribution network – Generating plants up to and including Type B, 2019"
- [3] Nederlandse Norm NEN-EN 50549-2, "Requirements for Generating plants to be connected in parallel with distribution networks – Part 2: Connection to a MV distribution network – Generating plants up to and including Type B, 2019"
- [4] D. Yoosefian, R. M. Chabanloo, "Protection of distribution network considering fault ride through requirements of wind parks", *Electric Power Systems Research* 178 (2020) 106019, 2020
- [5] Coster, E. J. (2010). *Distribution grid operation including distributed generation: impact on grid protection and the consequences of fault ride-through behavior*. PhD Thesis Technische Universiteit Eindhoven.
- [6] C. W. Taylor, "Power System Voltage Stability", 1994
- [7] T. V. Cutsem, C. Vournas, "Voltage Stability of Electric Power Systems", 1998
- [8] K. Amarasekara *et al.*, "Characterisation of Long-Term Voltage Stability with Variable-speed Wind Power Generation", *IET Generation Transmission & Distribution*, 2017
- [9] P. Kundur, "Power System Stability and Control", 1994
- [10] I. R. Navarro, "Dynamic Power System Load - Estimation of Parameters from Operational Data", PhD Thesis, Lund University
- [11] N. Save, M. Popov, A. Jongepier, G. Rietveld, "PMU-BASED POWER SYSTEM ANALYSIS OF A MV DISTRIBUTION GRID", *CIREC 24th International Conference on Electricity Distribution*, 2017
- [12] N. Save, "Phasor Measurement Unit based power system analysis of MV distribution grid", MSc Thesis, Delft University of Technology
- [13] DigSILENT PowerFactory, "User Manual" & "Technical Reference Documentation – Complex Load", 2018